



ORIGINAL ARTICLE

Network pharmacological analysis of the active molecules in *Coeloglossum viride* var. *bracteatum* and their anti-Alzheimer's disease activity through restoration of energy metabolism and inhibition of inflammation



Jin-Peng Bai^{a,1}, Jun Wang^{a,1}, Yang Hu^a, Qin Huang^a, Jing-Feng Dai^a, Guan-Li Xiao^b, Hui-Jing Yu^b, Xiao-Yan Qin^{a,*}, Rongfeng Lan^{b,*}

^a Key Laboratory of Ecology and Environment in Minority Areas National Ethnic Affairs Commission, Center on Translational Neuroscience, College of Life and Environmental Sciences, Minzu University of China, Beijing 100081, China

^b School of Pharmacy, Shenzhen University Health Science Center, Shenzhen 518060, China

Received 27 January 2023; accepted 13 May 2023

Available online 18 May 2023

KEYWORDS

Astrocyte;
BV2;
GFAP;
MAP2;
Glycolysis;
OXPHOS

Abstract *Coeloglossum viride* var. *bracteatum* is an advanced tonic in Tibetan medicine with anti-inflammatory and neuroprotective effects. Therefore, its anti-AD effects and potential targets should be explored. Firstly, a network pharmacological analysis of its bioactive molecules and their targets related to AD was performed, and the anti-inflammatory and energy metabolism modulating effects of its extract (CE) were investigated in LPS-induced astrocytes and BV2 cellular models. Then, inflammatory factors levels, ATP content and real-time energy metabolism were measured by RT-qPCR and Seahorse extracellular flux assays, respectively. Finally, we established a molecule-target network, as well as a PPI network of CE-related targets with AD-related targets, and identified 178 nodes and 2317 edges, yielding key targets that may play an important role in the treatment of AD. CE attenuated LPS-induced inflammation and apoptosis in astrocytes, while also enhancing energy metabolism in BV2 cells. Mechanistically, CE inhibited LPS-induced enhancement of microglia glycolytic activity and improved energy metabolism by inhibiting the HIF-1 α /PKM2 signaling axis. Thus, CE is a potential AD therapeutic agent with anti-inflammatory and energy metabolism modulating activities.

© 2023 The Author(s). Published by Elsevier B.V. on behalf of King Saud University. This is an open access article under the CC BY-NC-ND license (<http://creativecommons.org/licenses/by-nc-nd/4.0/>).

* Corresponding authors.

E-mail addresses: yang.hu@muc.edu.cn (Y. Hu), jingfengdai@sina.com (J.-F. Dai), bjqinxiaoyan@muc.edu.cn (X.-Y. Qin), lan@szu.edu.cn (R. Lan).

¹ These authors contribute equally: J-P Bai and J. Wang.

1. Introduction

Alzheimer's disease (AD), the most common cause of dementia, is a neurodegenerative disorder that constantly affects patients' memory and cognitive abilities (Knopman et al., 2021). AD is associated with deposition of extracellular amyloid- β protein (A β) plaques and intracellular tau-containing neurofibrillary tangles (NFTs), and thus accounts for 22.3% of clinical trials based on A β clearance (Liu et al., 2019, Knopman et al., 2021). However, the etiology and curative treatment of AD remain unclear. A growing body of evidence suggests that neuroinflammation may precede A β and tau lesions and that microglia play a crucial role (Heneka et al., 2015, Calsolaro and Edison 2016). In particular, microglia switching from a pro-inflammatory (M1) phenotype to an anti-inflammatory (M2) phenotype has been reported as a viable strategy for treating neuroinflammation (Zhang et al., 2018, Guo et al., 2022), and modulating this switch may be important for AD treatment, such as regulating the expression of AD risk gene Triggering Receptor Expressed on Myeloid cells 2 (TREM2) (Jiang et al., 2014), mutations in Toll-Like Receptors (TLRs) (Calsolaro and Edison 2016), and the metabolic shifts from oxidative phosphorylation (OXPHOS) to glycolysis (Pan et al., 2022). Furthermore, inhibition of glycolysis has been reported to ameliorate neuroinflammatory diseases associated with microglia activation (Cheng et al., 2021, Luo et al., 2021), specifically inhibition of Pyruvate Kinase M2 (PKM2) in AD (Pan et al., 2022). Therefore, modulating metabolic reprogramming in microglia inflammatory activation may be a promising therapeutic strategy for AD.

Traditional Chinese medicine, especially herbal medicines, has been reported to exert neuroprotective effects and improve cognitive function in AD through synergistic treatment with multiple components and targets (Zhao et al., 2020, Liu et al., 2021). The dried rhizome of *Coeloglossum viride* var. *bracteatum* has long been used as a Tibetan medicine for tranquilizing the mind and nourishing the qi, which has been documented in traditional Tibetan medical books such as "Jing Zhu Ben Cao" and "Si Bu Yi Dian" and the Pharmacopoeia of the People's Republic of China (Pharmacopoeia Committee of the P. R. China, 2020 edition) (Udo-Gendaan-Gompo 1983, Dilma-Tenzin-Phuntsok 2012). Therefore, it is also known in folklore as a miracle herb of immortality. Indeed, its bioactive components or extracts have been used in tonic drugs such as "Shi Wei Shou Shen San" and "Fu Fang Shou Shen Wan" approved by the National Medical Products Administration of China for the treatment of psychasthenia, debility and wasting (Shang et al., 2017, Huang et al., 2019). Previous works have identified over 120 chemicals in CE, including Militarine, Loriglossin, Dactylorhin A, Dactylorhin B, and Coelovirin A (Huang et al., 2004). For example, Dactylorhin B has been shown to have a detoxifying effect on A β -induced neurons (Zhang et al., 2006a, 2006b). Also, CE attenuates ischemia-induced neuronal death and cognitive dysfunction in rats (Ma et al., 2008) as well as toxin-induced memory impairment in mice (Zhang et al., 2006a, 2006b). We also found that CE ameliorated cognitive deficits and attenuated neurotoxicity in A β -induced AD mice and cellular models (Li et al., 2021, Li et al., 2022). Thus, these published works establish a proof of concept regarding the neuroprotective effects of CE and confirm its antipsychotic effects related to traditional functions. However, despite the initial understanding of the neuroprotective effects of CE, the pharmacological and molecular mechanisms of its multiple components are still not fully elucidated. Here, we applied the emerging approach of network pharmacology to understand the biological basis of network-based diseases and the network modulation mechanisms of herbal medicines (Wang et al., 2021), to investigate the therapeutic mechanisms of CE for AD in a holistic manner. We first employed a network pharmacology approach to predict the targets of CE and to establish an interaction network between CE-related targets and AD-related targets. Subsequently, we extracted a central target network and then performed enrichment analysis to find that CE may treat AD through anti-inflammation and regulation of energy metabolism.

Therefore, we established a cellular model of inflammation to confirm the results of the network pharmacological analysis and explore the underlying mechanisms, aiming to demonstrate that CE can alleviate inflammation and enhance the energy metabolism of microglia.

2. Materials and methods

2.1. Network pharmacology study

2.1.1. Target prediction and network construction for CE

The bioactive molecules of *Coeloglossum viride* var. *bracteatum* extract (CE) were derived from previous studies (Huang et al., 2004, Cai et al., 2021). Further information and screening of these molecules was obtained through the PubChem database (<https://pubchem.ncbi.nlm.nih.gov>) for the following analysis. Next, the Swiss Target Prediction database (<https://www.swisstargetprediction.ch>) was employed to predict the targets of all molecules via Canonical SMILES. Finally, a CE-molecule-target network was constructed with Cytoscape (version 3.7.2) to visualize and analyze the connections between herb, molecules and targets.

2.1.2. AD-related target collection

The GeneCards database (<https://www.genecards.org>), DisGeNET database (<https://www.disgenet.org>) and DrugBank (Law et al., 2014) database (<https://www.drugbank.ca>) were applied to obtain AD-related targets. All targets from these three databases were consolidated to remove duplicates and then submitted to the Uniprot database (<https://www.uniprot.org>) to normalize the names for gene and protein.

2.1.3. Protein-protein-interaction (PPI) network construction and key target clustering analysis of CE for AD

To evaluate and extract pivotal targets networks of CE for AD, we used BisoGenet (Martin et al., 2010) and CytoNCA applications (Tang et al., 2015) in Cytoscape (version 3.7.2) to build and analyze PPI networks. First, BisoGenet generates PPI networks for CE-associated targets and AD-associated targets, which are subsequently merged to create a crossover network. Then, the crossover network was computed and analyzed by CytoNCA to extract the hub target network with topological parameters including degree center (DC), local average connectivity-based approach (LAC), network center (NC), close to degree center (CC), and between degree centers (BC) (Zhang et al., 2020). Ultimately, gene clustering and corresponding Gene Ontology (GO) annotation was performed on targets in the extracted network by applying the Molecular Complex Detection (MCODE) algorithm (Bader and Hogue 2003) and GO in the Metascape online platform (<https://metascape.org>) (Zhou et al., 2019).

2.1.4. GO and KEGG pathway enrichment analysis

In addition to the annotation of gene clusters using Metascape, we performed gene enrichment analysis in the DAVID database (Sherman et al., 2022) (<https://david.ncifcrf.gov>) for all the targets extracted in Section 2.1.3, including gene ontology (GO) and Kyoto encyclopedia of genes and genomes (KEGG) pathway enrichment analysis. The results of GO enrichment analysis were visualized in <https://www.bioinformatics.com.cn>. The results of KEGG pathway enrichment analysis were visualized by the R platform (version 4.2.0).

2.2. Chemicals and reagents

Coeloglossum viride var. *bacteatum* extract (CE) was prepared and its composition was validated as previously described (Li et al., 2021). Lipopolysaccharides (LPS) was purchased from Solarbio (#L8880). WST-1 cell proliferation and cytotoxicity assay kit was purchased from Beyotime (#C0036L). *In situ* cell death detection kit for terminal deoxynucleotidyl transferase-mediated dUTP nick-end labelling (TUNEL) detection was purchased from Roche (#11684795910). The total RNA isolation kit was purchased from Beijing Zoman Biotechnology Co., Ltd (#ZP404).

2.3. Cell culture

To generate primary astrocytes and primary hippocampal neurons, the brains of neonatal Sprague-Dawley (SD) rats (provided by the Department of laboratory animal science of Peking University Health Science Center, license number SCXK-2011-0012) were dissected and the prefrontal-cortex and hippocampus were isolated. The isolated tissues were then digested (0.25% trypsin), filtered and centrifuged (1,100 rpm, 5 min) as previously described (Pan et al., 2017, Cai et al., 2021). Finally, astrocytes and neurons were cultured in DMEM medium containing 10% fetal bovine serum (FBS), 100 units/mL penicillin and 100 µg/mL streptomycin at 37 °C with 5% CO₂ for 7–10 days.

BV2 cells were provided by the Brain Science Center, Beijing Institute of Basic Medical Sciences and cultured in DMEM medium supplemented with 10% FBS, 100 units/mL penicillin and 100 µg/mL streptomycin at 37 °C with 5% CO₂ for 12 days.

2.4. Measurement of cell viability and apoptosis

The WST-1 assay was applied to measure cell viability. Briefly, after culturing and treating cells in 96-well plates with different conditions, 10 µL of WST-1 solution was added and incubated at 37 °C and 5% CO₂ for 1–2 h. Finally, the absorbance was recorded at 450 nm and the cell viability was calculated compared to the control absorbance.

Apoptosis was measured by the TUNEL assay according to the instructions of the *in situ* cell death assay kit. Briefly, cells were stained and observed under a fluorescent microscope. The rate of cell apoptosis was assessed by calculating the ratio of TUNEL/DAPI-positive cells.

2.5. Determination of inflammatory factors

The gene expression of inflammatory factors, including interleukin-6 (IL-6), interleukin-1β (IL-1β), tumor necrosis factor-α (TNF-α), and induced nitric oxide synthase 2 (Nos2, also known as iNOS), was examined by real-time quantitative polymerase chain reaction (RT-qPCR) experiments according to the instructions of the RNA kit. The sequences of the primers are listed as follows: *β-actin*, 5'-TGTCACCTTCCAG CAGA-3' (forward) and 5'-GCTCAGTAACAGTCCGCCT A-3' (reverse); *Il6*, 5'-ATTCTGTCTCGAGCCACCA-3'

(forward) and 5'-AGGCAACTGGCTGGAAGTCT-3' (reverse); *Il1β*, 5'-AATGCCTCGTGCTGTCTGA-3' (forward) and 5'-TGTCGTTGCTTGTCTCTCCT-3' (reverse); *Tnfα*, 5'-TGACCCCATTACTIONTCTGACC-3' (forward) and 5'-GGCC ACTACTTCAGCGTCTC-3' (reverse); *Nos2*, 5'-AAGA GACGCACAGGCAGAG-3' (forward) and 5'-CAGGCA CACGCAATGATGG-3' (reverse). Parameters for RT-qPCR cycles were set as follows. 120 s at 95 °C, 10 s at 95 °C (45 cycles), 95 °C for 10 s, 37 °C for 30 s. The relative expression levels of genes were calculated by the 2^{-ΔΔCt} method and normalized using β-actin as an internal control.

2.6. Immunofluorescence staining

Treated cells were seeded on 24-well plates, fixed with 4% paraformaldehyde for 15 min, and then incubated with 0.2% Triton X-100 for 10 min and blocked with PBS containing 10% goat serum. Cells were then incubated with the corresponding antibodies overnight and further immunofluorescence staining was performed at 4 °C. The primary antibodies were GFAP (#3670, Cell Signaling Technology), IBA1 (#019-19741, Wako, Japan) and MAP2 (#4542, Cell Signaling Technology). The secondary antibody used was Alexa Fluor 594-conjugated goat anti-rabbit IgG (#ZF-0513, ZSBG-Bio). DAPI was used to stain cell nuclei. Images of immunofluorescence staining were obtained using a Leica TCS SP8 confocal microscope.

2.7. ATP level measurements

The level of adenosine 5'-triphosphate (ATP) production in microglia reflects the metabolic pattern of energy (Cheng et al., 2014). Here, we added 100 µL of lysis buffer containing luciferase reagents (#G7570, Promega) to plates with cultured microglia for incubation. And then the plates were measured in a microplate reader and the luminescent signal was normalized.

2.8. Seahorse extracellular flux assay

The extracellular acidification rate (ECAR) and oxygen consumption rate (OCR) assays are based on the Seahorse XFe 96 Extracellular Flux Analyzer (Seahorse Bioscience), which reflects the real-time energy metabolism of the cells. All procedures conform to the instructions of the Seahorse XF Glycolysis Stress Test Kit (Agilent Technologies) and the Seahorse XF Cell Mito Stress Test Kit (Agilent Technologies). Briefly, microglia were seeded and treated in Seahorse XF-96-well plates under different conditions for 24 h. Microglia were then washed and maintained with XF assay medium for measurements. We first measured baselines. To measure ECAR, glucose (10 mM), oligomycin (oligo, 1 µM) and 2-deoxyglucose (2-DG, 50 mM) solutions were added sequentially to the Seahorse XF-96-well plates. To measure OCR, oligo (1 µM), *p*-trifluoromethoxy carbonyl cyanide phenylhydrazine (FCCP, 2 µM) and Rotenone/antimycin A (Rote/A, 0.5 µM) solutions were added sequentially. The results were normalized and analyzed by Seahorse XF 96 Wave software.

2.9. Western blotting

BV2 cells were harvested after treatment and subjected to protein extraction using RIPA buffer. Equal amounts of proteins were loaded onto SDS-PAGE and separated. Proteins were probed using specific primary antibodies for HIF-1 α (#bs-0737R) and PKM2 (#bs-0102 M), respectively. After incubation with HRP-conjugated secondary antibodies, protein signals were visualized by chemiluminescence in infrared fluorescence imaging system (Odyssey Clx, LI-COR Biosciences).

2.10. Data analysis

Experimental results were expressed as mean \pm s.e.m. Student's *t*-test and one-way analysis of variance (ANOVA) were applied to determine statistical differences between groups. Statistical analyses and plots were carried out in the software GraphPad Prism 8.0.

3. Results

3.1. Network pharmacological analysis of bioactive molecules in CE and potential AD-related targets.

Combining our previous study (Cai et al., 2021) and literature review (Huang et al., 2004, Zhang et al., 2006a, 2006b), we retrieved and finalized nine bioactive molecules that exhibit neuroprotective capacity as major ingredients of CE (Table 1). Among these nine molecules, Dactylorhin A, Dactylorhin B, Loriglossin, Militarine and Coelovirin A were shown to protect the nervous system from brain damage and cognitive impairment in animal models of AD and Parkinson's disease (PD) (Zhang et al., 2006a, 2006b, Pan et al., 2017, Li et al., 2021). Meanwhile, β -sitosterol was reported to improve memory and reduce amyloid-beta protein (A β) formation in APP/PSI mice (Wang et al., 2013, Ye et al., 2020), and Quercetin 3,7-diglucoside, Daucosterol and 4-Hydroxybenzaldehyde were shown to be antioxidants with potential neuroprotective capacity (Jiang et al., 2015, Oh et al., 2017, Sut et al., 2019). However, the manner and mechanism by which these nine molecules act together remains unknown. Here, we constructed a CE-molecules-targets network to demonstrate the linkage between these nine major components (Fig. 1A). Based on the molecules prediction targets in the Swiss Target Prediction database (Suppl. Table S1), the CE-molecule-target net-

work illustrates the distribution of targets, where 482 nodes represent targets and their network topology parameters represent relationships (Suppl. Table S2).

1017 CE-related targets were obtained from the GeneCards database, DisGeNET database and DrugBank database (Suppl. Table S3). To explore the key targets and protein interactions during CE treatment of AD, we built a PPI network of CE-related targets and AD-related targets using the BisoGenet program (Fig. 1B and 1C). In addition, a PPI network with a total of 178 nodes and 2317 edges was eventually screened (Fig. 1F), yielding the hub targets that may play an important role in the treatment of AD.

All topological parameters of the hub target PPI network were calculated in Cytoscape, by which we can rank the importance of the targets (Fig. 2A). The color and size of the nodes are proportional to their degrees in the network. For example, NPM1, HSPA5, HSPA8, EEF1A1 and HDAC5 may be critical nodes of great degree (Fig. 2A; Table S4). However, the application of network pharmacology emphasizes the synergistic effects of multiple targets at the overall system level (Yuan et al., 2017, Li 2021). Therefore, we applied the MCODE algorithm, an automated method for large protein interaction networks, to cluster and find molecular complexes (Bader and Hogue 2003). Seven clusters named "MCODE_" and their corresponding GO annotations were generated in Metascape (Fig. 2B and 2C). The GO terms of MCODE_5 and MCODE_7 are consistent with earlier studies (Pan et al., 2017, Li et al., 2021), describing that CE may treat AD by regulating oxidative stress and inflammation. In addition, the GO terms of MCODE_6 provide a new perspective focusing on energy metabolism.

Other than GO annotation of the clustered targets, we also performed GO enrichment analysis and KEGG pathway enrichment analysis to gain a comprehensive understanding of the biological functions of all 178 key targets (Fig. 3). As a result, pathways involved in inflammation were enriched, such as Toll-like receptor signaling pathway (hsa04620), TNF signaling pathway (hsa04668), NF-kappa B signaling pathway (hsa04064), MAPK signaling pathway (hsa04010) and IL-17 signaling pathway (hsa04657). Intriguingly, glycolysis/gluconeogenesis (hsa00010) was enriched in KEGG pathway analysis, while the GO terms ATP binding (GO: 0005524) and ATPase activity (GO: 0016887) were also found to be consistent with the clustering targets. Recent studies have proposed that AD progression can be accelerated by pro-inflammatory activation and aberrant glycolysis in different brain cell types, and targeting energy metabolism as well as inflammation may be a therapeutic strategy for AD (Tejera et al., 2019, Pan et al., 2022). Therefore, the

Table 1 Information on the nine active molecules in CE selected for network pharmacology analysis.

Molecules	Formula	Mw(g/mol)	CAS No.	Content (%)
Dactylorhin A	C ₄₀ H ₅₆ O ₂₂	888.9	256459-34-4	11.17
Dactylorhin B	C ₄₀ H ₅₆ O ₂₃	904.9	256459-36-6	7.82
Militarine	C ₃₄ H ₄₆ O ₁₇	904.9	58139-23-4	6.30
Loriglossin	C ₃₄ H ₄₆ O ₁₈	742.7	58139-22-3	11.00
Coelovirin A	C ₂₁ H ₃₀ O ₁₂	474.5	452963-01-8	n/a
Quercetin 3,7-diglucoside	C ₂₇ H ₃₀ O ₁₇	626.5	6892-74-6	n/a
β -Sitosterol	C ₂₉ H ₅₀ O	414.7	83-46-5	n/a
Daucosterol	C ₃₅ H ₆₀ O ₆	576.8	474-58-8	n/a
4-hydroxybenzaldehyde	C ₇ H ₆ O ₂	122.12	123-08-0	n/a

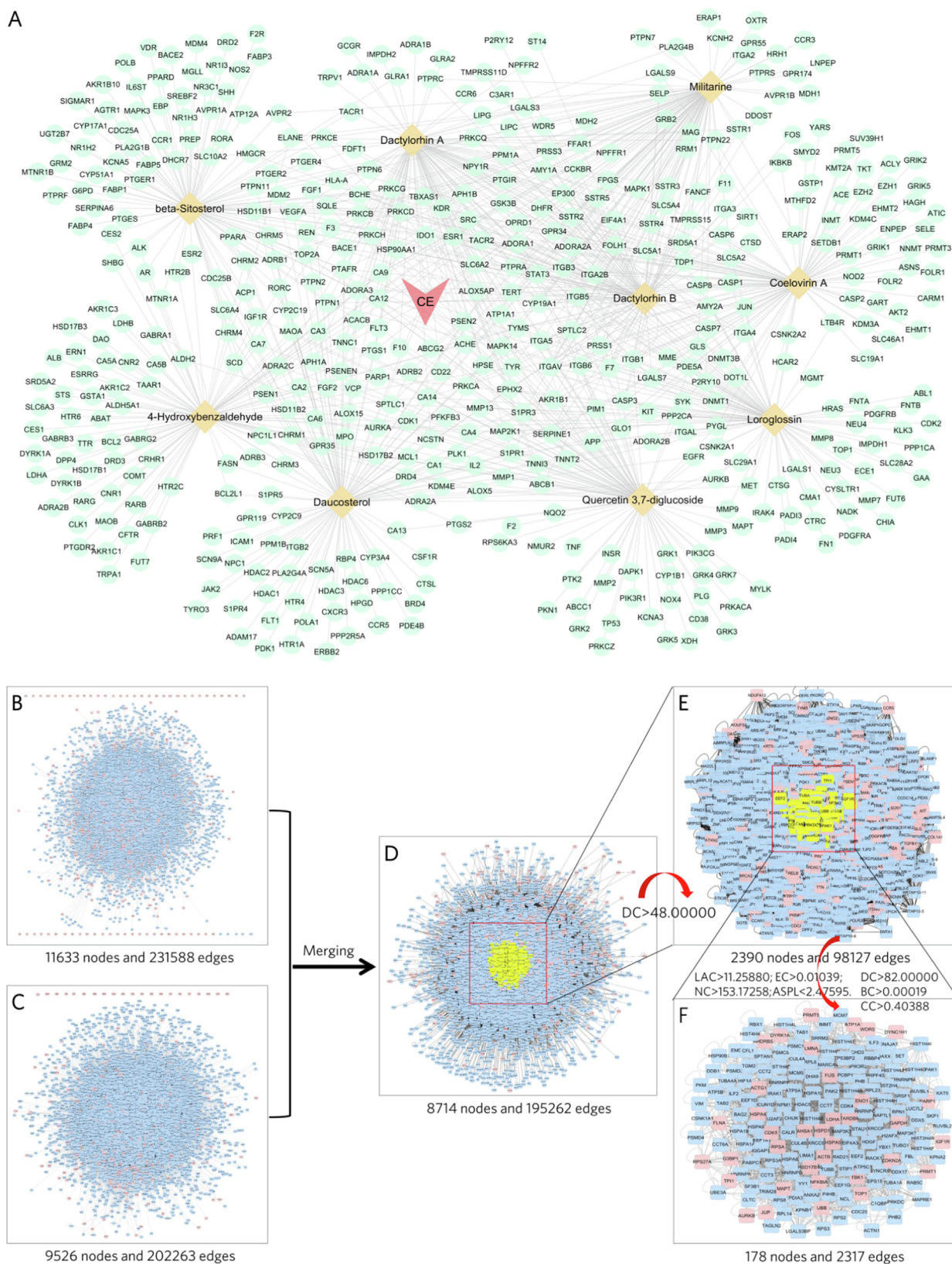


Fig. 1 Workflow of the PPI network used to construct the CE-molecules-targets network and extract the key targets. (A) In the CE-molecules-targets network, the aquamarine circles represent the putative targets of the corresponding molecules, the wheat colored diamonds represent the molecules in CE, the light pink triangles represents CE, and the edges represent the connections. (B) PPI network of AD-related targets. (C) PPI network of CE-related targets. (D) Crossover network after merging the AD-related PPI network and the CE-related PPI network. (E, F) PPI networks of key targets after filtering by topological parameters.

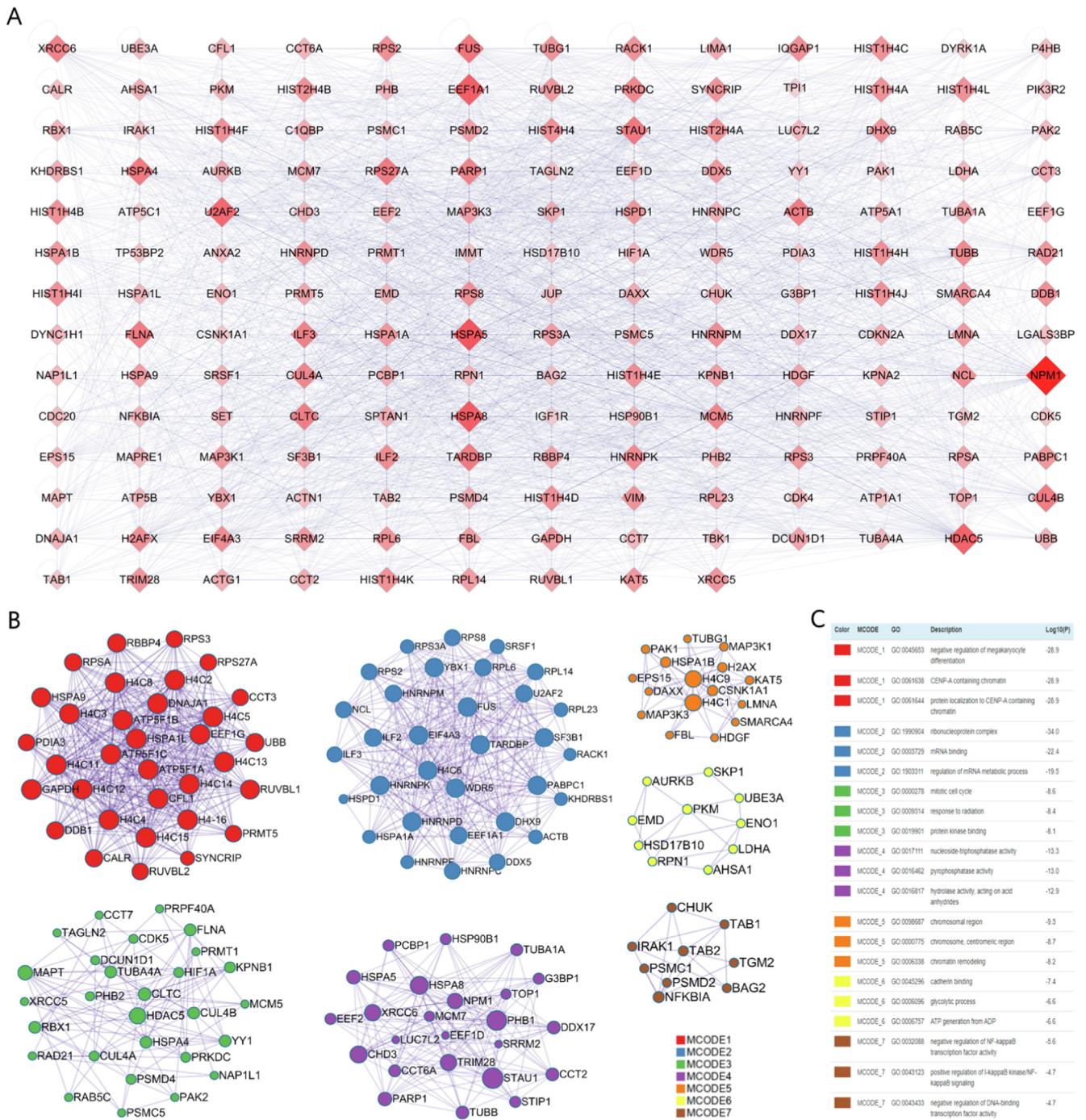


Fig. 2 Key target networks and gene clusters. (A) Key target network. The size and color of the diamonds are proportional to their degree centrality. (B, C) Modular description of the gene clusters and Metascape generated by the MCCODE algorithm.

results of the network pharmacology analysis suggest that CE may regulate inflammation and energy metabolism in AD, which is a promising finding.

3.2. CE attenuates LPS-induced inflammation in astrocytes and apoptosis in neurons

To confirm the results of the network pharmacology analysis that CE may regulate inflammation, we treated primary astrocytes and hippocampal neurons with LPS and CE, respec-

tively, while LPS is widely used to stimulate inflammation in cells (Calsolaro and Edison 2016). Cell viability was assessed with the WST-1 assay, and the expression levels of inflammatory factors were detected with RT-qPCR. The results showed that the cell viability of astrocytes decreased with increasing LPS concentration and the expression levels of TNF- α and IL-6 became higher (Fig. 4A and B), indicating that LPS managed to activate inflammation in astrocytes. Furthermore, since the 10 μ g/mL LPS-treated group had relatively low cell viability and higher expression levels of TNF- α and IL-6, we

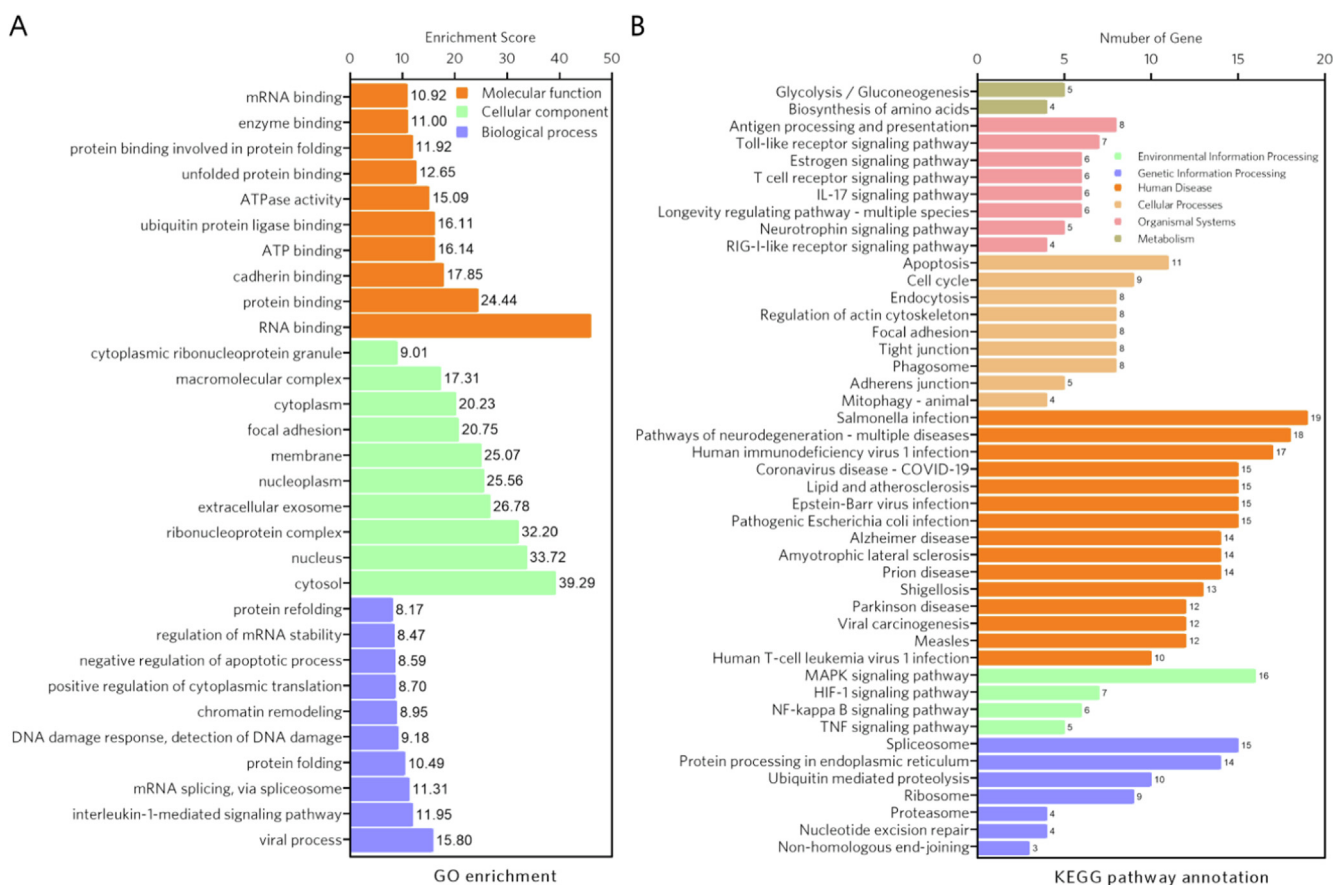


Fig. 3 GO enrichment analysis and KEGG pathway enrichment analysis of the hub targets. (A) GO enrichment analysis. The top ten GO terms were selected to describe the biological process (BP), cellular component (CC) and molecular function (MF) of the hub target. (B) KEGG pathway enrichment analysis. The pathways enriched in environmental information processing, genetic information processing, human disease, cellular processes, organismal systems, and metabolism were displayed.

selected this concentration of LPS to activate inflammation in these cell models in the next experiments. We next determined the anti-inflammatory effect of different concentration gradients of CE. The results demonstrated that treatment with CE, especially at 10 mg/mL, inhibited the LPS-induced decrease in cell viability and down-regulated the expression levels of inflammatory factor in astrocytes (Fig. 4A and B).

We also performed immunofluorescence to evaluate the morphological changes in cells treated with LPS and CE. Astrocytes activated by LPS for inflammation (labeled by GFAP) experienced a decrease in cell number and cell bodies, while astrocytes treated with CE, morphologically maintained their activity and size of the control (Fig. 4C). Similarly, CE improved the performance of neurons (labeled by MAP2) treated with LPS, showing greater cell numbers and neuronal connections (Fig. 4D). Consistent with this improvement, the results of the TUNEL assay showed an inhibitory effect of CE on LPS-induced neuronal apoptosis (Fig. 4E). Collectively, consistent with the results of the network pharmacology analysis, CE attenuated LPS-induced inflammation in astrocytes and neurons.

3.3. CE alleviates LPS-induced inflammation and enhances energy metabolism in microglia

Microglia-mediated neuroinflammation might contribute to the progression of AD, where the metabolic switching from

OXPHOS to aerobic glycolysis plays an important role (Leng and Edison 2021, Pan et al., 2022). Our network pharmacology analysis also provides evidence that CE may regulate energy metabolism against AD. Here, we used BV2 cells in various models to assay inflammatory factors and energy metabolism markers to elucidate whether CE could shift the metabolic patterns of activated microglia. In line with previous findings in astrocytes and neurons (Fig. 4), LPS activated inflammation in microglia (labeled by IBA1), while CE reduced activation (Fig. 5A). Quantitative data of activated cells were consistent with morphological findings (Fig. 5B), where activated microglia displayed larger size as well as abnormal shape (Fig. 5A). We also found that ATP levels were increased in the CE-treated group compared to the control or LPS-treated group (Fig. 5C). In addition, CE reduced the gene expression levels of inflammatory factors, including TNF- α , NOS2, IL-1 β , and IL-6 in LPS-treated microglia (Fig. 5D). Together, CE alleviated LPS-induced inflammation in microglia and promoted ATP expression, indicating that regulation of energy metabolism is involved in the anti-inflammatory effects of CE.

Furthermore, based on the results of the network pharmacology analysis and previous experiments, we cultured different microglia models to investigate the role of CE in metabolic regulation. The activation of microglia can be described as two phenotypes: M1 and M2 (Guo et al., 2022).

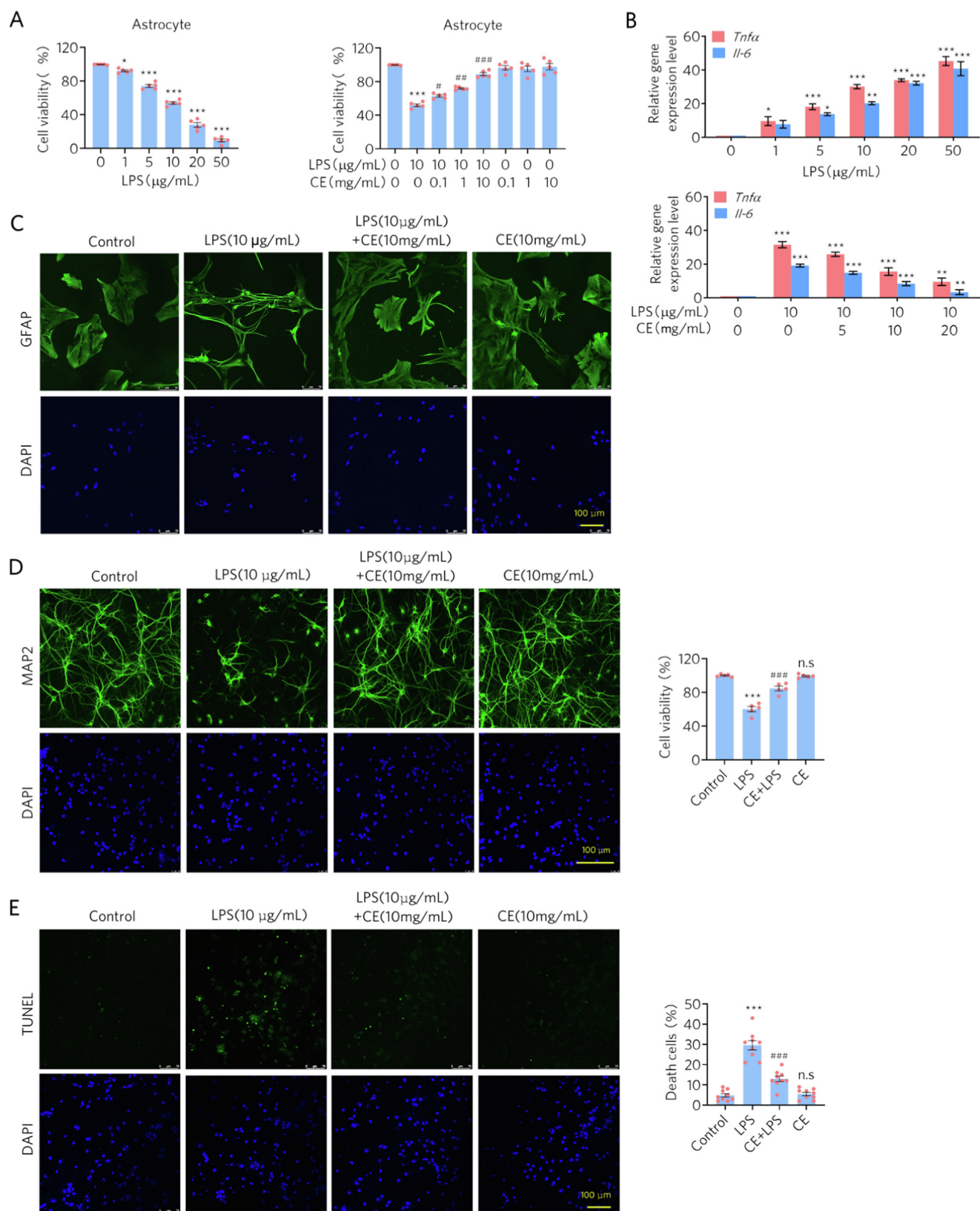


Fig. 4 CE attenuates LPS-induced inflammation in astrocytes and apoptosis in neurons. (A) CE rescued the cell viability of astrocytes from LPS treatment. Left, Student's *t* test was performed, $n = 5$, * $p < 0.05$, *** $p < 0.001$. Right, Student's *t* test was performed, $n = 5$, *** $p < 0.001$ versus control; # $p < 0.01$, ## $p < 0.005$, ### $p < 0.001$ versus 10 $\mu\text{g/mL}$ LPS. (B) CE down-regulated the expression levels of inflammatory factors in LPS-treated astrocytes. One-way ANOVA was performed, $n = 5$, * $p < 0.05$, ** $p < 0.01$, *** $p < 0.001$. (C) Immunofluorescence staining experiments showed morphological protection of CE against LPS on astrocytes. (D-E) Immunofluorescence staining experiments and TUNEL assays showed that CE protected the neurons from LPS-induced apoptosis. Student's *t* test was performed, $n = 9$, *** $p < 0.001$ (LPS vs Control), ### $p < 0.001$ (CE + LPS vs Control), n.s denotes not significant (CE vs Control).

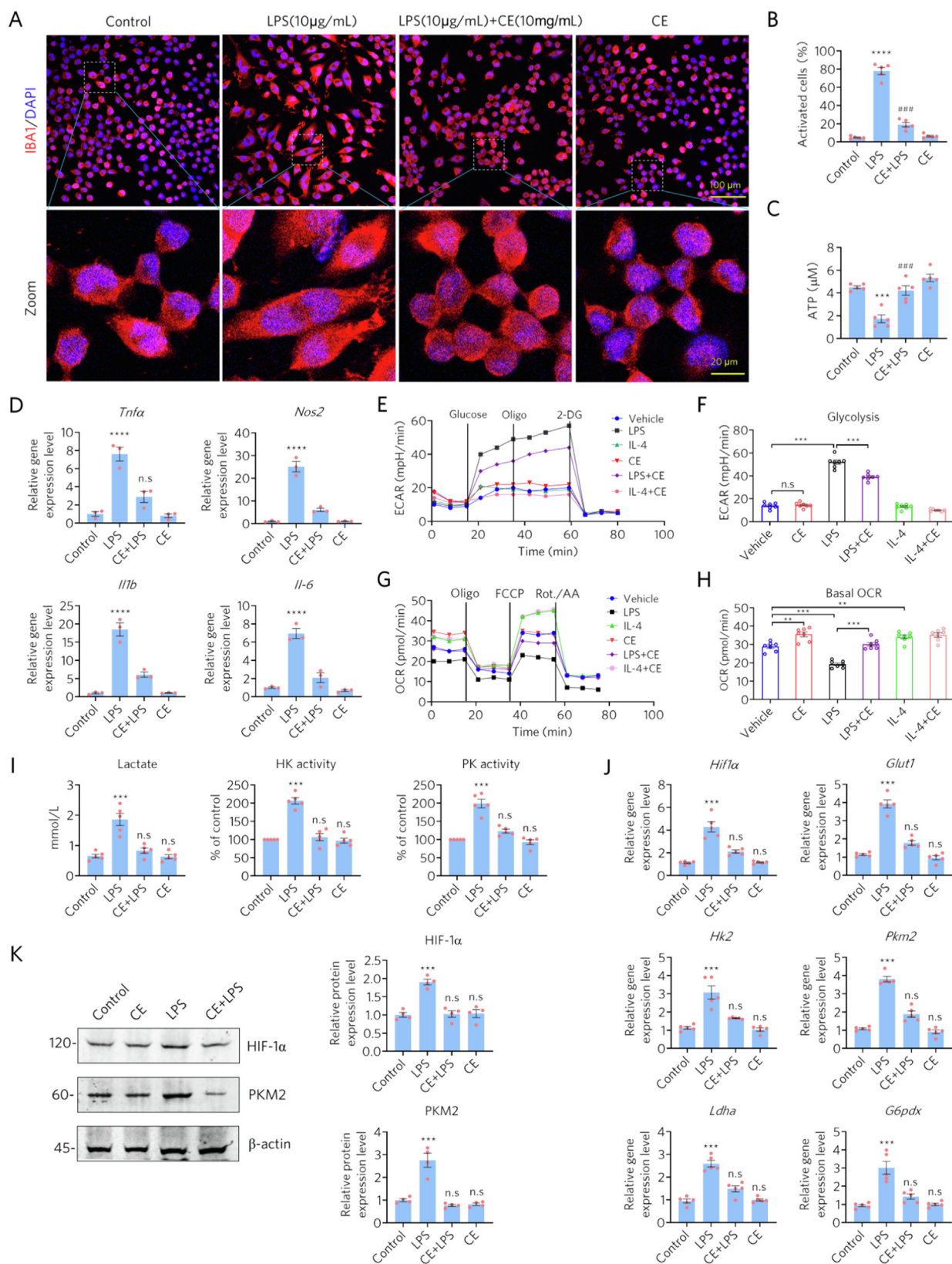


Fig. 5 CE alleviates LPS-induced inflammation and enhances energetic metabolism in microglia. (A-B) CE protected microglia from LPS-induced activation and morphological changes, $n = 5$. (C) CE rescued LPS-induced decrease of ATP, $n = 5$. (D) CE alleviated the LPS-induced elevation of gene expression in inflammatory factors, $n = 3$. (E-F) ECAR measurements of microglia. Oligo, oligomycin; 2-DG, 2-deoxyglucose. (G-H) OCR measurements of microglia. (I) Measurement of lactate production and the activities of HK and PK. (J) RT-qPCR assay of the gene expression levels of *Hif1 α* , *Glut1*, *Hk2*, and *Pkm2*. (K) Western blotting detects the protein levels of HIF-1 α and PKM2. The relative expression levels were normalized to β -actin. Student's *t*-test was performed in B, C, D, I, J, and K, **** $p < 0.001$ (LPS vs Control), #### $p < 0.001$ (CE + LPS vs LPS), n.s. denotes not significant. One-way ANOVA was performed in F and H, ** $p < 0.01$, *** $p < 0.001$, n.s., not significant.

M1 microglia exert pro-inflammatory effect leading to cell death, while M2 microglia protect neuronal cells from inflammation (Colonna and Butovsky 2017, Guo et al., 2022). Here, we treated microglia with LPS (LPS induces M1 polarization) or IL-4 (IL-4 induces M2 polarization) to induce microglia polarization and assessed the role of CE in both models. Energy metabolism, which includes ECAR and OCR related to cellular glycolysis and oxygenation, was examined with the Seahorse extracellular flux assay. The results showed that glycolysis in microglia was successfully enhanced by LPS but could be inhibited by CE (Fig. 5E and 5F), whereas CE had no effects on glycolysis in M2 microglia (IL-4-treated). In addition, OXPHOS was decreased in LPS-treated microglia, whereas CE reversed this phenomenon by promoting OXPHOS as in the IL-4-treated group (Fig. 5G and H). Therefore, CE can reprogram the metabolic state of microglia by regulating glycolysis and OXPHOS in different microglia models and promote the conversion of M1 microglia to M2 microglia.

We further examined the activity of hexokinase (HK) and pyruvate kinase (PK), as well as the levels of lactate. It was found that the activities of HK and PK were significantly increased in LPS-activated BV2 cells, accompanied by increased lactate production, which was reversed by CE (Fig. 5I). In addition, RT-qPCR assays for the expression of glycolysis-related genes, such as glucose transporter 1 (*Glut1*), hexokinase 2 (*Hk2*), lactate dehydrogenase A (*Ldha*), glucose-6-phosphate 1-dehydrogenase X (*G6pdx*) and M2-type pyruvate kinase (*Pkm2*), also confirmed that LPS significantly induced elevated expression levels of these genes (Fig. 5J). However, the elevated expression of LPS-activated microglia glycolysis-related genes was also restored by CE (Fig. 5J). Consistently, we also examined the changes in PKM2 and HIF-1 α protein levels, again confirming that CE reversed the LPS-induced elevation of PKM2 and HIF-1 α . These results suggest that CE inhibited the LPS-induced enhancement of microglia glycolytic activity and improved energy metabolism.

4. Discussion

Metabolic reprogramming plays a decisive role in the immune response and survival of immune cells. In the resting state, macrophages normally obtain their energy through mitochondrial oxidative phosphorylation (Kelly and O'Neill 2015). When they are activated to M1 type by LPS stimulation, cellular glucose metabolism shifts from oxidative phosphorylation to aerobic glycolysis, as evidenced by increased glucose uptake, increased lactate release, enhanced pentose phosphate pathway, decreased NAD⁺ content and reduced mitochondrial oxygen consumption, similar to the Warburg effect in tumor cells (Altenberg and Greulich 2004, Koppenol et al., 2011). Compared to mitochondrial OXPHOS, glycolysis produces more energy per unit time to meet the rapidly increasing ATP demand of macrophages due to biosynthesis, despite the low efficiency of glucose utilization (Pfeiffer et al., 2001). Macrophage M1 type activation resulted in high expression of *Glut1*, HK, PK, and lactate dehydrogenase (LDH), which promotes glycolysis, inhibits pyruvate dehydrogenase activity, prevents conversion of pyruvate to acetyl CoA, and ultimately inhibits the tricarboxylic acid cycle (Liu et al., 2012). The

molecular mechanisms underlying the shift from OXPHOS to aerobic glycolysis in inflammatory cells are still not fully elucidated. Interestingly, LPS induces an increased accumulation of succinate (an intermediate product of the tricarboxylic acid cycle) in macrophages, leading to increased stability of HIF-1 α protein and ultimately to enhance glycolysis and increased expression of the inflammatory factor IL-1 β , which is thought to be a key molecule in the transition from OXPHOS to aerobic glycolysis in inflammatory cells (Tannahill et al., 2013).

Furthermore, activation of PI3K/Akt/HIF-1 α signaling by LPS may be a key mechanism for the conversion of dendritic cells to aerobic glycolysis, while AMPK signaling has also been found to be involved in dendritic cell activation and aerobic glycolysis (O'Neill and Hardie 2013). As with peripheral macrophages, the transition of energy metabolism from oxidative phosphorylation to aerobic glycolysis occurs during M1-type activation of microglia in brain (Voloboueva et al., 2013, Orihuela et al., 2016). PKM2 serves as a key factor in regulating cellular metabolism and function, making it also important in regulating inflammation (O'Neill and Hardie 2013). In addition to being a key enzyme in the glycolytic process, PKM2 can also enter the nucleus as a dimer and bind to the promoters of HIF-1 α and IL-1 β to activate macrophages toward the M1 type and subsequently activate transcription of glycolysis-related genes, promoting the glycolytic process (Ouyang et al., 2018), while intracellular OXPHOS is significantly inhibited (Thompson et al., 2017). In this study, we found that the development of AD is closely related to inflammation and glycolysis through network pharmacological analysis, and the active ingredients of CE and their potential targets are associated with the development of AD and the regulation of inflammation and energy metabolism. Therefore, we suggest that CE bioactive molecules rich in antioxidant components can effectively inhibit inflammation and improve cellular energy status. In fact, in LPS-induced glial cell inflammatory activation and energy metabolism conversion cell models, we demonstrated that CE could effectively inhibit LPS-induced glial cell activation, prevent elevated expression of pro-inflammatory factors, and protect neuronal cells from inflammatory damage and apoptosis. Meanwhile, an M1-type shift in intracellular energy metabolism occurred due to LPS stimulation, with glucose catabolism shifting from OXPHOS to glycolytic predominance. However, active molecules of CE also inhibit this LPS-induced shift in energy metabolism, thus maintaining the balance of cellular energy metabolism.

Declaration of Competing Interest

The authors declare that they have no known competing financial interests or personal relationships that could have appeared to influence the work reported in this paper.

Acknowledgements

We thank the National Natural Science Foundation of China (81873088) and the First-class Undergraduate Course Construction Project of Minzu University of China (KC2210) for financial support.

Appendix A. Supplementary material

Supplementary data to this article can be found online at <https://doi.org/10.1016/j.arabjc.2023.105008>.

References

- Altenberg, B., Greulich, K.O., 2004. Genes of glycolysis are ubiquitously overexpressed in 24 cancer classes. *Genomics*. 84, 1014–1020. <https://doi.org/10.1016/j.ygeno.2004.08.010>.
- Bader, G.D., Hogue, C.W., 2003. An automated method for finding molecular complexes in large protein interaction networks. *BMC Bioinformatics*. 4, 2. <https://doi.org/10.1186/1471-2105-4-2>.
- Cai, Z.P., Cao, C., Guo, Z., et al, 2021. *Coeloglossum viride* var. *bacteatum* extract attenuates staurosporine induced neurotoxicity by restoring the FGF2-PI3K/Akt signaling axis and Dnmt3. *Heliyon* 7, e07503.
- Calsolaro, V., Edison, P., 2016. Neuroinflammation in Alzheimer's disease: Current evidence and future directions. *Alzheimers Dement*. 12, 719–732. <https://doi.org/10.1016/j.jalz.2016.02.010>.
- Cheng, S.C., Joosten, L.A., Netea, M.G., 2014. The interplay between central metabolism and innate immune responses. *Cytokine Growth Factor Rev*. 25, 707–713. <https://doi.org/10.1016/j.cytogfr.2014.06.008>.
- Cheng, J., Zhang, R., Xu, Z., et al, 2021. Early glycolytic reprogramming controls microglial inflammatory activation. *J Neuroinflammation* 18, 129. <https://doi.org/10.1186/s12974-021-02187-y>.
- Colonna, M., Butovsky, O., 2017. Microglia function in the central nervous system during health and neurodegeneration. *Annu Rev Immunol*. 35, 441–468. <https://doi.org/10.1146/annurev-immunol-051116-052358>.
- Dilma-Tenzin-Phuntsok, 2012. *Jing Zhu Ben Cao*. Shanghai Scientific and Technical Publishers, Shanghai. 10.1111/j.1474-9726.2012.00832.x.
- Guo, S., Wang, H., Yin, Y., 2022. Microglia polarization from M1 to M2 in neurodegenerative diseases. *Front. Aging Neurosci*. 14. <https://doi.org/10.3389/fnagi.2022.815347>
- Heneka, M.T., Carson, M.J., El Khoury, J., et al, 2015. Neuroinflammation in Alzheimer's disease. *Lancet Neurol*. 14, 388–405. [https://doi.org/10.1016/S1474-4422\(15\)70016-5](https://doi.org/10.1016/S1474-4422(15)70016-5).
- Huang, T., Danaher, L.A., Bruschweiler, B.J., et al, 2019. Naturally occurring bisphenol F in plants used in traditional medicine. *Arch Toxicol*. 93, 1485–1490. <https://doi.org/10.1007/s00204-019-02442-5>.
- Huang, S.Y., Li, G.Q., Shi, J.G., et al, 2004. Chemical constituents of the rhizomes of *Coeloglossum viride* var. *bacteatum*. *J Asian Nat Prod Res*. 6, 49–61. <https://doi.org/10.1080/1028602031000119826>.
- Jiang, T., Yu, J.T., Zhu, X.C., et al, 2014. Triggering receptor expressed on myeloid cells 2 knockdown exacerbates aging-related neuroinflammation and cognitive deficiency in senescence-accelerated mouse prone 8 mice. *Neurobiol Aging*. 35, 1243–1251. <https://doi.org/10.1016/j.neurobiolaging.2013.11.026>.
- Jiang, L.H., Yuan, X.L., Yang, N.Y., et al, 2015. Daucosterol protects neurons against oxygen-glucose deprivation/reperfusion-mediated injury by activating IGF1 signaling pathway. *J. Steroid Biochem. Mol. Biol*. 152, 45–52. <https://doi.org/10.1016/j.jsbmb.2015.04.007>.
- Kelly, B., O'Neill, L.A., 2015. Metabolic reprogramming in macrophages and dendritic cells in innate immunity. *Cell Res*. 25, 771–784. <https://doi.org/10.1038/cr.2015.68>.
- Knopman, D.S., Amieva, H., Petersen, R.C., et al, 2021. Alzheimer disease. *Nat. Rev Dis. Primers* 7, 33. <https://doi.org/10.1038/s41572-021-00269-y>.
- Koppenol, W.H., Bounds, P.L., Dang, C.V., 2011. Otto Warburg's contributions to current concepts of cancer metabolism. *Nat Rev Cancer*. 11, 325–337. <https://doi.org/10.1038/nrc3038>.
- Law, V., Knox, C., Djombou, Y., et al, 2014. DrugBank 4.0: shedding new light on drug metabolism. *Nucleic Acids Res*. 42, D1091–D1097. <https://doi.org/10.1093/nar/gkt1068>.
- Leng, F., Edison, P., 2021. Neuroinflammation and microglial activation in Alzheimer disease: where do we go from here? *Nat Rev Neurol*. 17, 157–172. <https://doi.org/10.1038/s41582-020-00435-y>.
- Li, S., 2021. Network pharmacology evaluation method guidance - draft. *World J. Traditional Chinese Med*. 7, 146–154. https://doi.org/10.4103/wjtc.wjtc_11_21.
- Li, X.-X., Cai, Z.-P., Lang, X.-Y., et al, 2021. *Coeloglossum viride* var. *bacteatum* extract improves cognitive deficits by restoring BDNF, FGF2 levels and suppressing RIP1/RIP3/MLKL-mediated neuroinflammation in a 5xFAD mouse model of Alzheimer's disease. *J. Functional Foods* 85. <https://doi.org/10.1016/j.jff.2021.104612>.
- Li, X.X., Lang, X.Y., Ren, T.T., et al, 2022. *Coeloglossum viride* var. *bacteatum* extract attenuates Abeta-induced toxicity by inhibiting RIP1-driven inflammation and necroptosis. *J. Ethnopharmacol*. 282. <https://doi.org/10.1016/j.jep.2021.114606>
- Liu, T.F., Vachharajani, V.T., Yoza, B.K., et al, 2012. NAD⁺-dependent sirtuin 1 and 6 proteins coordinate a switch from glucose to fatty acid oxidation during the acute inflammatory response. *J Biol Chem*. 287, 25758–25769. <https://doi.org/10.1074/jbc.M112.362343>.
- Liu, P.P., Xie, Y., Meng, X.Y., et al, 2019. History and progress of hypotheses and clinical trials for Alzheimer's disease. *Signal Transduct. Target Ther*. 4, 29. <https://doi.org/10.1038/s41392-019-0063-8>.
- Liu, N., Zhang, T., Sun, J., et al, 2021. An overview of systematic reviews of chinese herbal medicine for Alzheimer's Disease. *Front. Pharmacol*. 12. <https://doi.org/10.3389/fphar.2021.761661>
- Luo, G., Wang, X., Cui, Y., et al, 2021. Metabolic reprogramming mediates hippocampal microglial M1 polarization in response to surgical trauma causing perioperative neurocognitive disorders. *J. Neuroinflammation* 18, 267. <https://doi.org/10.1186/s12974-021-02318-5>.
- Ma, B., Li, M., Nong, H., et al, 2008. Protective effects of extract of *Coeloglossum viride* var. *bacteatum* on ischemia-induced neuronal death and cognitive impairment in rats. *Behav. Pharmacol*. 19, 325–333. <https://doi.org/10.1097/FBP.0b013e3282feb0ac>.
- Martin, A., Ochagavia, M.E., Rabasa, L.C., et al, 2010. BisoGenet: a new tool for gene network building, visualization and analysis. *BMC Bioinformatics* 11, 91. <https://doi.org/10.1186/1471-2105-11-91>.
- Oh, S.H., Ryu, B., Ngo, D.H., et al, 2017. 4-hydroxybenzaldehyde-chito oligomers suppresses H2O2-induced oxidative damage in microglia BV-2 cells. *Carbohydr Res*. 440–441, 32–37. <https://doi.org/10.1016/j.carres.2017.01.007>.
- O'Neill, L.A., Hardie, D.G., 2013. Metabolism of inflammation limited by AMPK and pseudo-starvation. *Nature* 493, 346–355. <https://doi.org/10.1038/nature11862>.
- Orihuela, R., McPherson, C.A., Harry, G.J., 2016. Microglial M1/M2 polarization and metabolic states. *Br. J. Pharmacol*. 173, 649–665. <https://doi.org/10.1111/bph.13139>.
- Ouyang, X., Han, S.N., Zhang, J.Y., et al, 2018. Digoxin suppresses pyruvate kinase M2-Promoted HIF-1 α transactivation in steatohepatitis. *Cell Metab*. 27 (339–350), e333.
- Pan, R.Y., Ma, J., Wu, H.T., et al, 2017. Neuroprotective effects of a *Coeloglossum viride* var. *bacteatum* extract in vitro and in vivo. *Sci. Rep*. 7, 9209. <https://doi.org/10.1038/s41598-017-08957-0>.
- Pan, R.Y., He, L., Zhang, J., et al, 2022. Positive feedback regulation of microglial glucose metabolism by histone H4 lysine 12 lactylation in Alzheimer's disease. *Cell Metab*. 34 (634–648), e636.
- Pfeiffer, T., Schuster, S., Bonhoeffer, S., 2001. Cooperation and competition in the evolution of ATP-producing pathways. *Science* 292, 504–507. <https://doi.org/10.1126/science.1058079>.
- Shang, X., Guo, X., Liu, Y., et al, 2017. *Gymnadenia conopsea* (L.) R. Br.: a systemic review of the ethnobotany, phytochemistry, and

- pharmacology of an important asian folk medicine. *Front. Pharmacol.* 8, 24.
- Sherman, B.T., Hao, M., Qiu, J., et al, 2022. DAVID: a web server for functional enrichment analysis and functional annotation of gene lists (2021 update). *Nucleic Acids Res.* <https://doi.org/10.1093/nar/gkac194>.
- Sut, S., Dall'Acqua, S., Poloniato, G., et al, 2019. Preliminary evaluation of quince (*Cydonia oblonga* Mill.) fruit as extraction source of antioxidant phytoconstituents for nutraceutical and functional food applications. *J. Sci. Food Agric.* 99, 1046–1054. <https://doi.org/10.1002/jsfa.9271>.
- Tang, Y., Li, M., Wang, J., et al, 2015. CytoNCA: a cytoscape plugin for centrality analysis and evaluation of protein interaction networks. *Biosystems* 127, 67–72. <https://doi.org/10.1016/j.biosystems.2014.11.005>.
- Tannahill, G.M., Curtis, A.M., Adamik, J., et al, 2013. Succinate is an inflammatory signal that induces IL-1beta through HIF-1alpha. *Nature*. 496, 238–242. <https://doi.org/10.1038/nature11986>.
- Tejera, D., Mercan, D., Sanchez-Caro, J.M., et al, 2019. Systemic inflammation impairs microglial Abeta clearance through NLRP3 inflammasome. *EMBO J.* 38. <https://doi.org/10.15252/embj.2018101064>.
- Thompson, A.A., Dickinson, R.S., Murphy, F., et al, 2017. Hypoxia determines survival outcomes of bacterial infection through HIF-1alpha dependent re-programming of leukocyte metabolism. *Sci Immunol.* 2. <https://doi.org/10.1126/sciimmunol.aal2861>.
- Udo-Gendaan-Gompo, 1983. *Si Bu Yi Dian*. People's Health Publishing House, Beijing. 10.1111/j.1474-9726.2012.00832.x.
- Voloboueva, L.A., Emery, J.F., Sun, X., et al, 2013. Inflammatory response of microglial BV-2 cells includes a glycolytic shift and is modulated by mitochondrial glucose-regulated protein 75/mortalin. *FEBS Lett.* 587, 756–762. <https://doi.org/10.1016/j.febslet.2013.01.067>.
- Wang, X., Wang, Z.Y., Zheng, J.H., et al, 2021. TCM network pharmacology: a new trend towards combining computational, experimental and clinical approaches. *Chin. J. Nat. Med.* 19, 1–11. [https://doi.org/10.1016/S1875-5364\(21\)60001-8](https://doi.org/10.1016/S1875-5364(21)60001-8).
- Wang, J., Wu, F., Shi, C., 2013. Substitution of membrane cholesterol with beta-sitosterol promotes nonamyloidogenic cleavage of endogenous amyloid precursor protein. *Neuroscience*. 247, 227–233. <https://doi.org/10.1016/j.neuroscience.2013.05.022>.
- Ye, J.Y., Li, L., Hao, Q.M., et al, 2020. beta-Sitosterol treatment attenuates cognitive deficits and prevents amyloid plaque deposition in amyloid protein precursor/presenilin 1 mice. *Korean J. Physiol. Pharmacol.* 24, 39–46. <https://doi.org/10.4196/kjpp.2020.24.1.39>.
- Yuan, H., Ma, Q., Cui, H., et al, 2017. How can synergism of traditional medicines benefit from network pharmacology? *Molecules* 22. <https://doi.org/10.3390/molecules22071135>.
- Zhang, D., Liu, G., Shi, J., et al, 2006a. Coelloglossum viride var. bracteatum extract attenuates D-galactose and NaNO₂ induced memory impairment in mice. *J. Ethnopharmacol.* 104, 250–256. <https://doi.org/10.1016/j.jep.2005.09.010>.
- Zhang, T., Pan, L., Cao, Y., et al, 2020. Identifying the mechanisms and molecular targets of Yizhiqingxin formula on Alzheimer's Disease: coupling network pharmacology with GEO database. *Pharmgenomics Pers Med.* 13, 487–502. <https://doi.org/10.2147/PGPM.S269726>.
- Zhang, B., Wei, Y.Z., Wang, G.Q., et al, 2018. Targeting MAPK pathways by naringenin modulates microglia M1/M2 polarization in lipopolysaccharide-stimulated cultures. *Front. Cell Neurosci.* 12, 531. <https://doi.org/10.3389/fncel.2018.00531>.
- Zhang, D., Zhang, Y., Liu, G., et al, 2006b. Dactylorhin B reduces toxic effects of beta-amyloid fragment (25–35) on neuron cells and isolated rat brain mitochondria. *Naunyn Schmiedebergs Arch Pharmacol.* 374, 117–125. <https://doi.org/10.1007/s00210-006-0095-9>.
- Zhao, J., Lan, X., Liu, Y., et al, 2020. Anti-aging role of Chinese herbal medicine: an overview of scientific evidence from 2008 to 2018. *Ann Palliat Med.* 9, 1230–1248. <https://doi.org/10.21037/apm.2020.04.09>.
- Zhou, Y., Zhou, B., Pache, L., et al, 2019. Metascape provides a biologist-oriented resource for the analysis of systems-level datasets. *Nat. Commun.* 10, 1523. <https://doi.org/10.1038/s41467-019-09234-6>.